ORIGINAL ARTICLE

Regional Alterations in Cortical Sulcal Depth in Living Fetuses with Down Syndrome

Hyuk Jin Yun[1,2], Juan David Ruiz Perez[1,2], Patricia Sosa[1,2],
J. Alejandro Valdés[1,2], Neel Madan[3], Rie Kitano[4], Shizuko Akiyama[4],
Brian G. Skotko[5], Henry A. Feldman[2,6], Diana W. Bianchi[7], P. Ellen Grant[1,2,8],
Tomo Tarui[4] and Kiho Im[1,2]

[1]Fetal Neonatal Neuroimaging and Developmental Science Center, Boston Children's Hospital, Harvard Medical School, Boston, MA 02115, USA, [2]Division of Newborn Medicine, Boston Children's Hospital, Harvard Medical School, Boston, MA 02115, USA, [3]Department of Radiology, Tufts Medical Center, Boston, MA 02111, USA, [4]Mother Infant Research Institute, Tufts Medical Center, Boston, MA 02111, USA, [5]Down Syndrome Program, Genetics, Pediatrics, Massachusetts General Hospital, Boston, MA 02114, USA, [6]Institutional Centers for Clinical and Translational Research, Boston Children's Hospital, Harvard Medical School, Boston, MA 02115, USA, [7]Prenatal Genomics and Fetal Therapy Section, Medical Genetics Branch, National Human Genome Research Institute, Bethesda, MD 20892, USA and [8]Department of Radiology, Boston Children's Hospital, Harvard Medical School, Boston, MA 02115, USA

Address correspondence to Kiho Im, PhD, Fetal-Neonatal Neuroimaging and Developmental Science Center, Division of Newborn Medicine, Boston Children's Hospital, 300 Longwood Ave, Boston, MA 02115, USA. Email: Kiho.Im@childrens.harvard.edu.
Drs Tarui and Im serve as equally contributing senior authors

Abstract

Down syndrome (DS) is the most common genetic cause of developmental disabilities. Advanced analysis of brain magnetic resonance imaging (MRI) has been used to find brain abnormalities and their relationship to neurocognitive impairments in children and adolescents with DS. Because genetic factors affect brain development in early fetal life, there is a growing interest in analyzing brains from living fetuses with DS. In this study, we investigated regional sulcal folding depth as well as global cortical gyrification from fetal brain MRIs. Nine fetuses with DS (29.1 ± 4.24 gestational weeks [mean ± standard deviation]) were compared with 17 typically developing [TD] fetuses (28.4 ± 3.44). Fetuses with DS showed lower whole-brain average sulcal depths and gyrification index than TD fetuses. Significant decreases in sulcal depth were found in bilateral Sylvian fissures and right central and parieto-occipital sulci. On the other hand, significantly increased sulcal depth was shown in the left superior temporal sulcus, which is related to atypical hemispheric asymmetry of cortical folding. Moreover, these group differences increased as gestation progressed. This study demonstrates that regional sulcal depth is a sensitive marker for detecting alterations of cortical development in DS during fetal life, which may be associated with later neurocognitive impairment.

Key words: cortical folding, Down syndrome, fetal brain, magnetic resonance imaging, sulcal depth

Introduction

Down syndrome (DS), also known as trisomy 21, is a genetic disease that affects one out of 700 live births (CDC 2019; Mai et al. 2019). Although the neuropathology is still not fully understood, patients with DS have distinctive features such as craniofacial dysmorphology and neurocognitive impairment (Palisano et al. 2001; Lee et al. 2016; Hamner et al. 2018; Baburamani et al. 2019; Rodrigues et al. 2019). People with DS show mild to severe intellectual disabilities that manifest in early childhood. Impairments in the domains of behavior, language, and verbal/visual/spatial memory are thought to be closely related to abnormal brain growth (Marcell 1995; Chapman and Hesketh 2001; Pinter et al. 2001; Vicari 2006; Losin et al. 2009; Jacola et al. 2014).

Quantitative approaches using brain magnetic resonance imaging (MRI) have been used to characterize abnormal brain development in individuals with DS. Using MRI volumetric analysis, many studies revealed that children with DS have smaller brain sizes compared with typically developing (TD) children (Pinter et al. 2001; Menghini et al. 2011; Lee et al. 2016; Hamner et al. 2018; Baburamani et al. 2019; Rodrigues et al. 2019). Regional volume reduction has also been reported in several areas such as frontal, temporal, and medial occipital lobes, Sylvian fissure, gray and white matters, and cerebellum (Pinter et al. 2001; Rigoldi et al. 2009; Carducci et al. 2013; Lee et al. 2016; Hamner et al. 2018). These anatomical changes in DS have been associated with neurocognitive impairment. Decreased gray matter density in the orbitofrontal cortex and temporal lobe regions have been related to long-term memory deficits (Menghini et al. 2011; Hamner et al. 2018). The impairment of short-term memory was associated with gray matter reduction in the Sylvian fissure, superior temporal gyrus, and medial occipital lobe (Menghini et al. 2011; Carducci et al. 2013; Hamner et al. 2018). Volume reduction in the cerebellar vermis was related to the low quality of gating (Rigoldi et al. 2009). Furthermore, atypical patterns of functional network activation in children with DS have been reported. In fact, immature development of functional connectivity in DS was found to be associated with impaired aggregation of information between brain regions (Anderson et al. 2013). Abnormal functional activation was shown in DS compared with normal subjects in the middle and superior temporal gyri, which are related to auditory and language processing (Losin et al. 2009; Jacola et al. 2014). Among the various brain regions in previous studies, the Sylvian fissure and temporal regions have been frequently reported as both structural and functional abnormalities.

The abovementioned imaging abnormalities in DS are considered to originate from abnormal early brain development, influenced by an abnormal genomic environment caused by trisomy 21. Previous studies following fetopsy reported volume reduction in the temporal lobe and cerebellum, which may be due to decreased neurogenesis and abnormal neuronal differentiation, along with increased apoptosis during fetal brain development (Golden and Hyman 1994; Guihard-Costa et al. 2006; Guidi et al. 2008, 2018; Bhattacharyya et al. 2009; Kanaumi et al. 2013). Recently, our in vivo MRI study allowed global brain volumetric and surface area analysis in living fetuses with DS (Tarui et al. 2020). We identified different growth patterns in the cortical plate, subcortical parenchymal, and cerebellar volumes as well as in the hemispheric surface area between fetuses with DS and TD fetuses in the second half of gestation (Tarui et al. 2020). Another study has also found consistent atypical brain development in fetuses with DS (Patkee et al. 2020). Therefore,

analyzing fetal brains may provide a better understanding of the regional onset of abnormal brain development in DS and therefore provide hints as to the genetic mechanisms involved.

In contrast to atypical volumetric and global area brain growth, little is known about alterations of cortical folding in fetuses with DS. Cortical folding is an important aspect of in utero neurodevelopment as its pattern is prenatally determined and under strong genetic controls (Rubenstein and Rakic 1999; Piao et al. 2004; Rakic 2004; O'Leary et al. 2007; Kostovic and Vasung 2009; Hill et al. 2010; White et al. 2010; Chen et al. 2012; Stahl et al. 2013; Miller et al. 2014). Atypical cortical folding can result from defects in neuronal proliferation, migration, and differentiation and is associated with neurocognitive impairment in many brain malformations and disorders (Molko et al. 2003; Rakic 2004; Nakamura et al. 2007; Cykowski et al. 2008). Furthermore, there is a region-specific timing of the emergence of primary cortical folding during the fetal stage (Garel et al. 2003; Habas et al. 2012; Yun et al. 2020). Since regional cortical surface growth and folding are associated with the development of specific functional areas (Rakic 1988; Welker 1990; Zilles et al. 1997; Hasnain et al. 2001; Eickhoff et al. 2006; Fischl et al. 2008; Ronan and Fletcher 2015), examining regional cortical folding has provided more information about region-specific functional development that is not captured by whole-brain global analysis (Germann et al. 2005, 2019; Nordahl et al. 2007; Cykowski et al. 2008; McKay et al. 2013; Leroy et al. 2015; Lefèvre et al. 2016). Quantitative and regional analysis of cortical folding in fetuses with DS may lead to a better understanding of early abnormalities in brain development, the mechanisms underlying pathological changes and specific neurocognitive impairment in DS.

The aim of this study is to evaluate differences in global and regional cortical folding between fetuses with DS and TD fetuses during the second half of gestation. To measure quantitative features of cortical folding, we extracted hemispheric surface models of the fetal brains and calculated sulcal depth and gyrification index (GI). First, we globally compared whole-brain average sulcal depth and GI between the two groups. Then, sulcal depth at each vertex of the surface models was analyzed to detect regional alterations in fetuses with DS. We hypothesized that significantly altered sulcal depth and GI would be found in DS fetuses at both global and regional levels.

Materials and Methods

Subjects and Image Acquisition

The use of fetal MRIs was approved by the institutional review boards of participating institutions at Boston Children's Hospital (BCH) and Tufts Medical Center (TMC). Nine fetuses with DS (gestational weeks [GW]: 29.1 ± 4.24 (mean $\pm$ standard deviation), range: 21.7–35.1; sex: 4/5 [male/female]) used in our previous study (Tarui et al. 2020) were included in this study. At TMC, eight pregnant women whose fetuses were prenatally suspected or diagnosed with DS were prospectively recruited. Prenatal diagnosis of DS was suspected by maternal plasma positive cell-free DNA screening results or a diagnostic fetal karyotype obtained by amniocentesis (AC) or chorionic villus sampling. All newborns without a confirmed prenatal diagnosis were confirmed with a postnatal karyotype. Prenatal and postnatal diagnoses of major anomalies were also recorded (Table 1). One fetus with DS was added from the retrospective patient data at BCH.

Seventeen TD GW-matched controls (GW: 28.4 ± 3.44, range: 22.0–32.0; sex: 7/10) were collected from prior prospective recruitment studies, which included TD fetuses as controls at BCH and TMC, and clinical fetal MRIs performed to screen for abnormalities at BCH. Inclusion criteria for TD fetuses included no serious maternal medical conditions (nicotine or drug dependence, morbid obesity, cancer, diabetes, and gestational diabetes), and maternal age between 18 and 45 years. Exclusion criteria of TD fetuses included multiple gestation pregnancies, dysmorphic features on ultrasound (US) examination, brain malformations/lesions or other identified organ anomalies on US examination, known chromosomal abnormalities, known congenital infections, and any abnormality on the fetal MRI. Between the DS and TD groups, we found no significant differences in GW at scan ($P = 0.650$), which was assessed by an independent t-test or sex ratio ($P = 0.952$) yielded by a chi-squared test. Maternal and fetal information of all the fetuses is shown in Table 1.

Fetal brain MRIs were acquired on a Siemens 3 T Skyra scanner (BCH) or Philips 1.5 T scanner (TMC) using a T2-weighted Half-Fourier Acquisition Single-Shot Turbo Spin-Echo (HASTE) sequence with 1 mm in-plane resolution, FOV = 256 mm, time repetition = 1.5 s (BCH) or 12.5 s (TMC), time echo = 120 ms (BCH) or 180 ms (TMC), and slice thickness = 2–4 mm. After localizing the fetal brain, totally 3–10 HASTE scans were acquired multiple times in three different orthogonal orientations (scan time for acquisition of volumetric images was 10–20 min) for reliable image head motion correction and 3D reconstruction of fetal brain MRI. A part of this multi-center TD subject data has been used in our prior studies in which we addressed relatively less influence of scanner effect in extracting cortical folding measures (Tarui et al. 2018) and no significant differences in the accuracy of automatic sulcal labeling method between the fetal subjects from different scanners (Yun et al. 2019).

MRI Processing and Surface Reconstruction

To extract cortical surfaces, we adopted our pipeline for fetal MRI processing (Im et al. 2017; Tarui et al. 2018; Yun et al. 2019, 2020). The overview of the pipeline is shown in Figure 1. Combining multiple 2D slices of fetal brain MRI with a slice to volume super-resolution technique (Kuklisova-Murgasova et al. 2012), we created a motion-corrected 3D volume with 0.75 mm isotropic resolution. Then, a semi-automatic approach based on voxel intensity was applied to the 3D volume for segmenting cortical plate. To minimize the noise of the segmentation, we spatially smoothed the inner volume of the segmented cortical plate using 1.5 mm full width at half-maximum (FWHM) kernel. On the smoothed volume, the hemispheric (left and right) triangular surface meshes were extracted by a function "isosurface" in MATLAB 2018b (MathWorks Inc., Natick, MA). Geometrical smoothing was performed to reduce the noise and small geometric changes of the surface models were performed using Freesurfer (https://surfer.nmr.mgh.harvard.edu). For vertex-wise statistical analysis, the smoothed cortical surface was aligned to a template surface using a 2D sphere-to-sphere warping method (Robbins 2004; Robbins et al. 2004; Boucher et al. 2009). The non-rigid warping method searches optimal correspondences of vertices using folding similarity between two surfaces. We selected as a registration target a 28 GW template surface created from similarly reconstructed T2 MRI volumes in a different TD fetal cohort (Serag et al. 2012; Yun et al. 2019). In our previous study, we demonstrated that

surface registration between the 28 GW template and individual fetal brain surfaces at different GW (from 22 to 32 GW) is highly reliable (Yun et al. 2019).

Cortical Sulcal Depth and GI

On the cortical surface, we measured sulcal depth. In order to calculate sulcal depth, we used the adaptive distance transform (ADT) method developed from our previous study (Yun et al. 2013). The ADT was proposed as an optimal algorithm for measuring sulcal depth, which showed superior robustness against complicated cortical shape and sensitivity to structural changes of the human brain. The basic concept of the ADT is to search for the shortest path from the convex hull to the cortical surface. To obtain the convex hull, we performed a morphological closing operation with a 10 mm spherical kernel on the inner cortical plate volume and defined the convex hull as edge voxels of the closed volume. Then, a 3D Cartesian coordinate system, named local coordinates, was created in the space between the convex hull and cortical surface. For each vertex of the cortical surface, the shortest path from the convex hull was generated in the local coordinates using the Dijkstra algorithm. The length of the shortest path was calculated as sulcal depth of each vertex. To eliminate noise, we smoothed the sulcal depth of cortical surface with a 10 mm FWHM Gaussian kernel. Individual maps of the smoothed sulcal depth on the cortical surfaces are shown for all subjects in Supplementary Figure 1. Additionally, whole-brain average depth from all vertices was calculated as a global feature.

In addition to sulcal depth, we also computed GI, which is a global feature representing the magnitude of cortical convolution. The definition of GI is the area ratio between the cortical surface and the convex hull (Zilles et al. 1988; Harris et al. 2004; Gaser et al. 2006; Schaer et al. 2006). We extracted the convex hull surface from the closed volume described above and calculated the global GI of the whole-brain.

Statistical Analysis

Because one of the fetuses had two MRIs at different gestational ages, we employed a linear mixed model for group comparison between TD and DS fetuses. Linear mixed models are an extension of linear regression models that contain both fixed and random effects (Baltagi 2008). A random effect is frequently used for longitudinal or repeated data that correlate between observations. Matrix formulation of our linear mixed model is represented as follows:

$$Y = \beta X + uZ + \varepsilon,$$

where Y is an observation vector, β represents regression coefficients of a matrix of fixed effects (X), u indicates covariate vector for the design matrix for random effects (Z), and ε is random errors. In the linear mixed model, sulcal depth or GI was observation; group information was fixed effect, and subject ID was random effect. In the model, we added GW to the matrix of fixed effects for adjusting the dynamic changes of cortical folding in early fetal life (Clouchoux et al. 2012; Yun et al. 2020). Using the linear mixed model, we globally and regionally analyzed the features. Whole-brain average sulcal depth and GI were used as global features. For the regional analysis, sulcal depth in each vertex was independently analyzed, and false discovery rate

Table 1 Maternal and fetal information of fetuses with DS and TD controls used in this study

	Subject ID	Maternal age and risk[a]	CVS, AC, postnatal karyotype	Fetal sex M: male F: female	GW at scan	Other anomalies
DS	Subject 1	30	47, XX, +21	F	30.9	None
	Subject 2	33	47, XX, +21	M	31.6	None
	Subject 3	30	47, XX, +21	F	29.7	AVCD repaired after birth
	Subject 4	41	47, XX, +21	F	30.9	AVCD repaired after birth
	Subject 5[b]	33	47, XX, +21	F	22.3[a] and 29.7[b]	ASD, mitral regurgitation, PFO repaired after birth
	Subject 6	36	47, XX, +21	M	21.7	Neonatal pulmonary hypertension
	Subject 7	34	47, XX, +21	F	35.1	None
	Subject 8	44	47, XX, +21	M	27.4	Interrupted aortic arch repaired after birth, hydronephrosis
TD	Subject 9	38[a]	47, XX, +21	M	32.4	Tricuspid regurgitation
	Subject 10	30	N/A	M	29.6	None
	Subject 11	32	N/A	F	22.9	None
	Subject 12	22	N/A	F	29.1	None
	Subject 13	33	N/A	F	25.6	None
	Subject 14	34	N/A	M	32.0	None
	Subject 15	34	N/A	M	24.7	None
	Subject 16	28	N/A	F	29.6	None
	Subject 17	29	N/A	M	28.6	None
	Subject 18	34	N/A	F	31.4	None
	Subject 19	35	N/A	F	30.9	None
	Subject 20	29	N/A	M	30.3	None
	Subject 21	40	N/A	F	30.7	None
	Subject 22	30	N/A	F	29.4	None
	Subject 23	28	N/A	F	31.6	None
	Subject 24	41	N/A	F	31.7	None
	Subject 25	29	N/A	M	22.6	None
	Subject 26	33	N/A	M	22.0	None

ASD, atrial septal defect; AVCD, atrioventricular canal defect; CVS, chorionic villi sampling; PFO: patent foramen ovale.

[a]Maternal risks—Cymbalta, Lyrica for fibromyalgia.

[b]Longitudinal data (a: baseline scan, and b: follow-up scan). DS subject 5 has two scans at different GW (subject 5a [22.3 GW] and 5b [29.7 GW]). Note: There is no significant group difference in GW (P = 0.650) or sex ratio (P = 0.952). All the fetuses with DS and a part of TD were used in our previous study (Tarui et al. 2020).
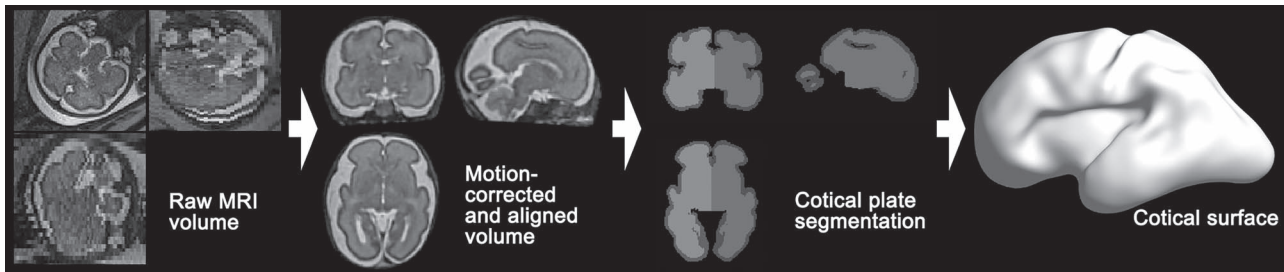
Figure 1. Overview of fetal brain MRI processing pipeline for cortical surface reconstruction. Raw MRI volume of fetal brain is processed for motion-correction and spatial alignment. Left and right cortical plate regions are segmented, and then cortical surface is extracted.

(FDR) correction was applied to correct multiple comparisons problem. We set the significance level of FDR-corrected P value to 0.05 from the linear mixed model. To examine group differences in age-related trajectories of sulcal depth and GI, group-GW interaction term was added as a fixed effect in the linear mixed model.

For the regions with significant group difference in sulcal depth, we analyzed hemispheric asymmetry of sulcal depth. Leftward asymmetry indices of sulcal depth were calculated by the following equation:

$$\text{Asymmetry} = 2 \times \left(D_{\text{left}} - D_{\text{right}}\right) / \left(D_{\text{left}} + D_{\text{right}}\right),$$

where D_{left} and D_{right} are sulcal depth in the left and right hemispheres, respectively. Positive asymmetry indices indicate that the left hemisphere has larger sulcal depth compared with the right hemisphere and vice versa. We also examined age-related averaged mean curvature changes in the regions with significant group difference to observe subtle changes of cortical folding. The sign of mean curvature indicates inwardly folded (negative) or outwardly folded (positive) regions (Meyer et al. 2003). Mean curvature was computed by the angular deviation from a patch around each vertex. Then, the mean curvature was smoothed with 10 mm FWHM kernel on the cortical surface. The linear mixed model was applied to test the group difference of the sulcal depth asymmetry index and mean curvature between TD and DS fetuses. We also compared group differences in age-related trajectories of asymmetries and mean curvature by adding group-GW interaction term in the linear mixed model.

In addition, we performed supplementary experiments: 1) since there was only one subject that had two MRI scans at different GW, we used a subset of fetuses excluding the follow-up scan and compared group differences in regional sulcal depth using a simple linear regression model and (2) we added cerebral volume and scanner as covariates in the linear mixed model to control for brain size and scanner effects in the group comparison. We adjusted GW and applied FDR correction in the supplementary experiments.

Results

In the linear mixed model, fetuses with DS showed significantly lower whole-brain average sulcal depth ($P = 0.003$) and GI ($P = 0.009$) than TD fetuses. Significantly different age-related trajectories of whole-brain average sulcal depth ($P = 0.006$) and GI ($P = 0.008$) were also found (Fig. 2). The difference of whole-brain sulcal depth and GI was increased as gestation progressed. The results of the regional comparison of sulcal depth between

the groups using the linear mixed model are shown in Figure 3. Fetuses with DS showed significantly shallower sulcal depth (FDR-corrected $P < 0.05$) compared with TD fetuses in multiple cortical regions, especially in the bilateral Sylvian fissure, right central, and parieto-occipital sulci. In contrast to others, a region belonging to the left superior temporal sulcus showed significantly deeper sulcal depth in fetuses with DS compared with TD fetuses.

To assess the regional differences in the age-related trajectory of sulcal depth between DS and TD groups, we segmented the cortical regions in which significant group difference in sulcal depth was found. The vertices in the significant regions were clustered via connected component clustering approach. Among the clusters, we selected five clusters whose area is over 0.1% of the total surface area (Fig. 4A). Like vertex-wise results, significant group differences ($P < 0.001$) in average sulcal depth were found in all the clusters: bilateral Sylvian fissure, left superior temporal, right central, and parieto-occipital sulci. The age-related sulcal depth changes in these regions are shown in Figure 4B. In all the clusters, sulcal depth differences between the two groups were gradually increased as gestation progressed, and significant interaction terms were found in the bilateral Sylvian fissures ($P < 0.001$ [left], and $P = 0.001$ [right]), left superior temporal sulcus ($P = 0.011$), and right central sulcus ($P < 0.001$) (Fig. 4B). However, the interaction term was not statistically significant in parieto-occipital sulcus ($P = 0.231$).

In the leftward asymmetry index analysis, we found that fetuses with DS showed a significantly larger leftward asymmetry in the superior temporal sulcus compared with TD fetuses ($P = 0.014$) using the linear mixed model. In contrast to the superior temporal sulcus, there was no significant group difference in the Sylvian fissure ($P = 0.232$), central ($P = 0.267$) and parieto-occipital sulci ($P = 0.130$). The age-related trajectory of asymmetry indices in the regions are shown in Figure 4C. A significant group-GW interaction term was only found in the superior temporal sulcus ($P = 0.026$). In the mean curvature analysis, fetuses with DS showed less inward folding (higher mean curvature) in the bilateral Sylvian fissure ($P = 0.001$ [left], and $P < 0.001$ [right]), right central ($P < 0.001$), and parieto-occipital sulci ($P < 0.001$) than TD fetuses (Supplementary Fig. 2). Same as sulcal depth, mean curvature in the left superior temporal sulcus ($P < 0.001$) showed inverse pattern compared with that in other regions (Supplementary Fig. 2). Furthermore, group differences in age-related trajectories of mean curvature were found in bilateral Sylvian fissure ($P = 0.014$ [left], and $P < 0.001$ [right]), left superior temporal ($P = 0.042$), and right central sulci ($P < 0.001$).

The result of the supplementary experiment using the subset without the follow-up scan was consistent with the main
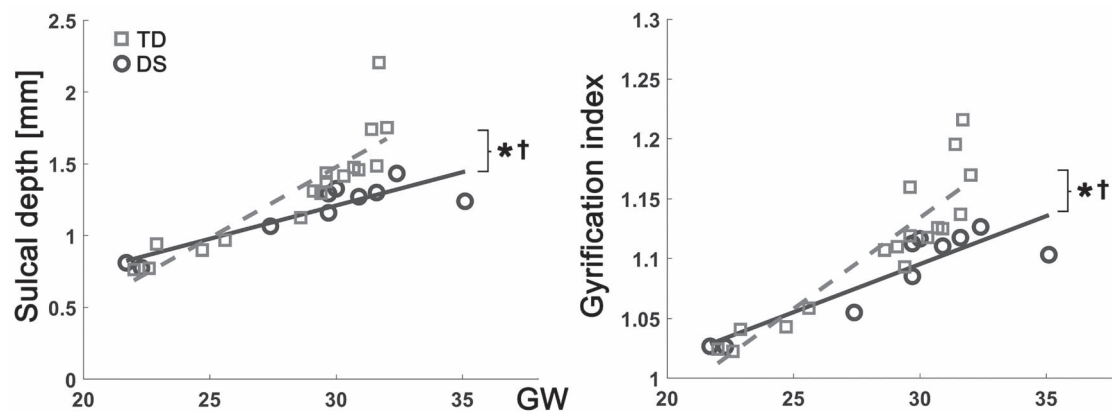
Figure 2. Growth trajectories of whole brain average sulcal depth and GI. x-axis indicates GW, and y-axis indicates observed values of sulcal depth (mm) and GI. *Significant group difference and †significant group-GW interaction effect.
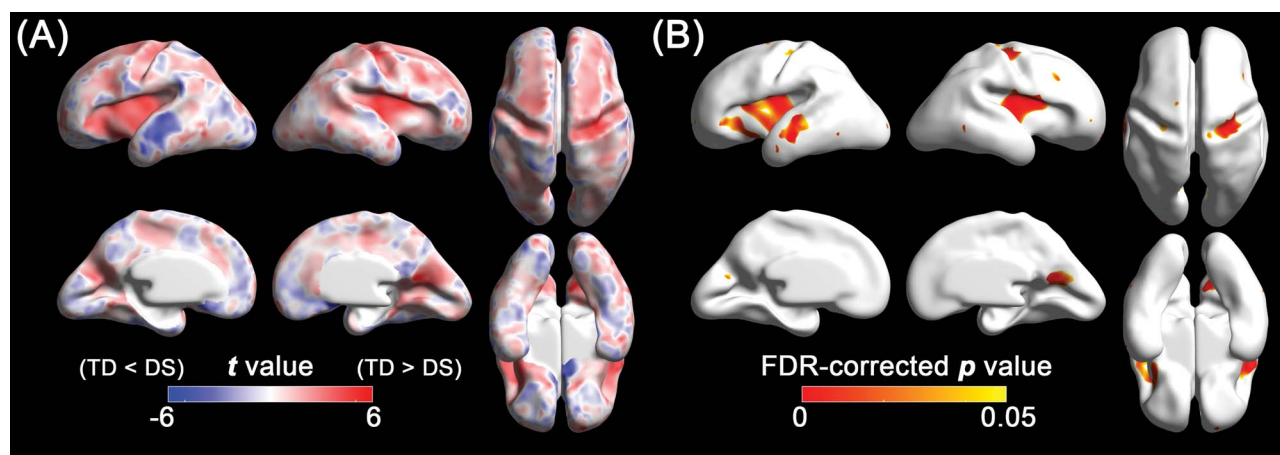

Figure 3. Statistical results of the vertex-wise comparison in sulcal depth between DS and TD fetuses using the linear mixed models. (A) Statistical t map. Red indicates sulcal depth in fetuses with DS is shallower than TD fetuses, and blue indicates sulcal depth in fetuses with DS is deeper than TD fetuses. (B) FDR-corrected p map. Red represents regions showing statistically different sulcal depth between DS and TD groups (FDR-corrected P < 0.05).

result (Fig. 3), showing significant sulcal depth differences (FDR-corrected P < 0.05) in the Sylvian fissure, left superior temporal, right central, and parieto-occipital sulci (Supplementary Fig. 3). Adding cerebral volume and scanner effects as covariates in the linear mixed models, significant group difference (FDR-corrected P < 0.05) in sulcal depth were also found in the Sylvian fissure, left superior temporal, right central and parieto-occipital sulci (Supplementary Fig. 4).

Discussion

In this study, we quantitatively evaluated the differences in cortical folding between fetuses with DS and TD fetuses in the second half of pregnancy. We used sulcal depth and GI which have shown high sensitivity in detecting abnormal cortical folding (Ramenghi et al. 2007; Dubois et al. 2008; Engelhardt et al. 2015; Shimony et al. 2016). The findings of sulcal depth and GI support our hypothesis that cortical folding in the fetuses with DS significantly differs from that of TD controls.

Fetuses with DS showed smaller whole-brain average sulcal depth and GI than TD fetuses. In the human brain, cortical folding is thought to be associated with rapid cortical

expansion in functional areas that results from neurogenesis and neuronal proliferation in ventricular and subventricular zones during early fetal life (Chenn and Walsh 2002; O'Leary et al. 2007; Rakic 2009; Lui et al. 2011; Sun and Hevner 2014). Existing evidence from human fetopsies and animal model studies suggests that aberrant brain development in DS begins during fetal life. The process of neurogenesis is severely impaired in DS, due to a reduction in the size of the pool of neural progenitor cells starting from the beginning of brain development (Guidi et al. 2008; Bhattacharyya et al. 2009; Stagni et al. 2018). This reduction is caused by decreased proliferation rate (due to a longer cell cycle), precocious exit from the cell cycle (fewer rounds of division occur), and increased apoptotic cell death. Impaired neurogenesis and neuronal proliferation by genetic defects in DS may reduce cortical surface expansion and cause altered cortical folding during fetal life. Although these brain abnormalities originate in early fetal life, altered cortical folding development may be related to future neurodevelopmental impairments in DS children.

Not only did we find global differences, we also found several cortical regions with significantly altered sulcal development from early fetal stages. Fetuses with DS showed significant
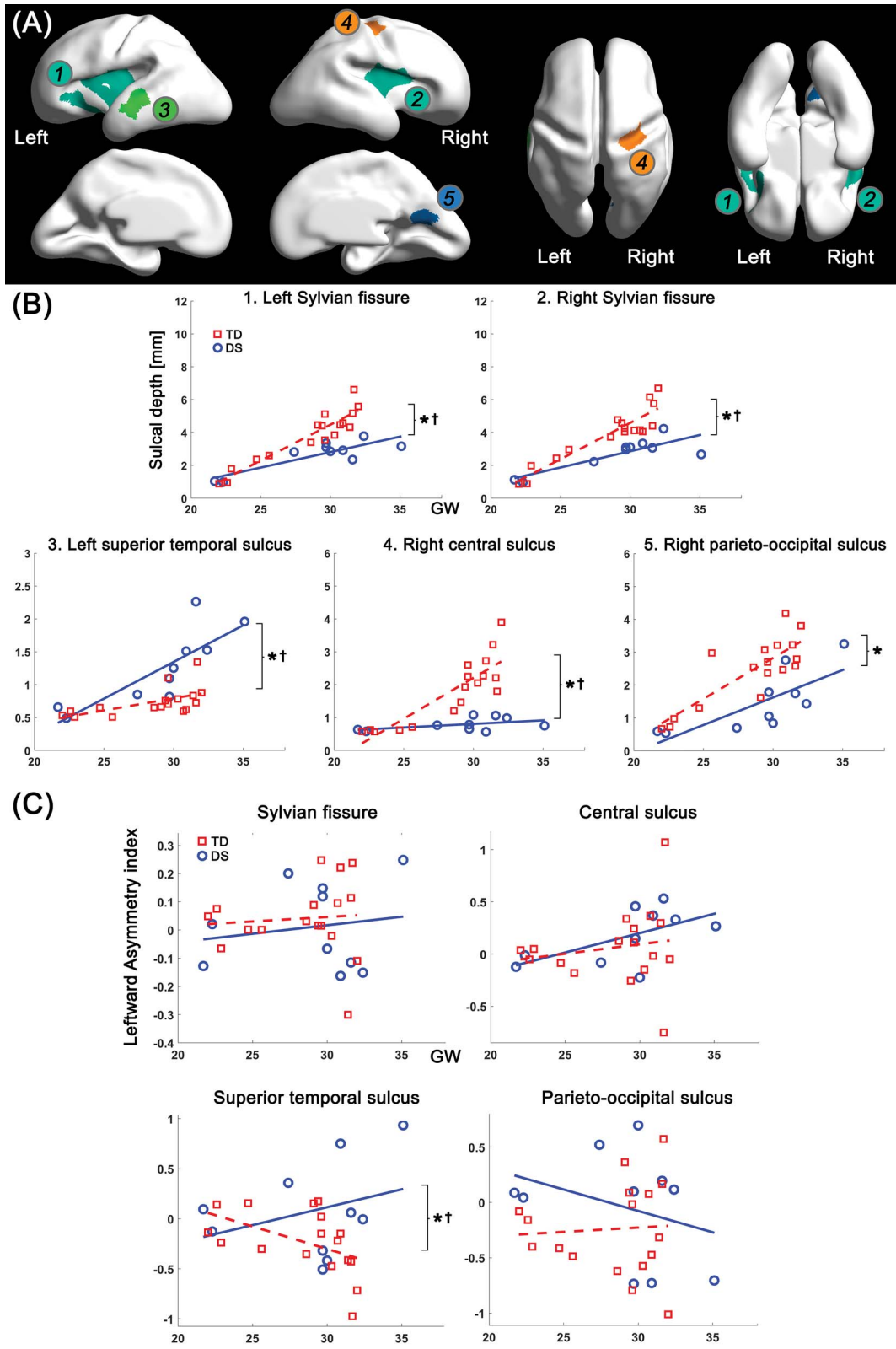
Figure 4. Clustered regions showing significant group difference in sulcal depth, and age-related trajectories of sulcal depth and leftward asymmetry index in the regions. (A) Clustered regions under 0.05 of FDR-corrected P value in group comparison. The clusters belong to 1) left Sylvian fissure, 2) right Sylvian fissure, 3) left superior temporal sulcus, 4) right central sulcus, and 5) right parieto-occipital sulcus. (B) Growth trajectories of average sulcal depth and their group difference in each cluster. (C) Age-related changes of leftward asymmetry index and their group difference in each cluster. x-axis indicates GW, and y-axis indicates observed values of sulcal depth (mm) and leftward asymmetry index. *Significant group difference and †significant group-GW interaction effect.

shallower sulcal depth in the bilateral Sylvian fissure, right central, and parieto-occipital sulcus, compared with TD fetuses. These regions belong to the early emerging sulci (Garel et al. 2001, 2003; Habas et al. 2012; Yun et al. 2020). Shallow sulcal depth in the Sylvian fissure bilaterally is supported by previous studies reporting brain abnormalities and developmental delay in the Sylvian fissure of children with DS (Menghini et al. 2011; Carducci et al. 2013). Abnormalities in the fetal Sylvian fissure may be associated with abnormal development of the operculum (described as operculization process) and developmental delay (Chen et al. 1996; Guibaud et al. 2008; Lerman-Sagie and Malinger 2008). Findings in the right central sulcus may be associated with the motor abnormalities in children with DS that have been reported in several studies (Davis and Kelso 1982; Palisano et al. 2001; Vicari 2006). Significantly shallow sulcal depth in the right parieto-occipital sulcus is consistent with previous studies that revealed gray matter reduction in the medial part of occipital lobe in DS children (Menghini et al. 2011; Hamner et al. 2018). In contrast to other regions, significantly deeper sulcal depth in the superior temporal sulcus was found in fetuses with DS. Interestingly, temporal regions have been frequently reported as abnormal in previous studies. Volume reduction in the temporal lobe, especially in the superior and middle temporal gyrus, has been reported in DS (Pinter et al. 2001; Kates et al. 2002; Menghini et al. 2011; Carducci et al. 2013; Lee et al. 2016). In fetopsy, altered development of neuronal cells in the temporal lobe was revealed (Golden and Hyman 1994; Kanaumi et al. 2013). Our findings of deeper left superior temporal sulcus in fetuses with DS might be explained by different asymmetry patterns compared with TD fetuses. In TD human brains, the left superior temporal sulcus has a slower sulcal emergence (Dubois et al. 2008; Habas et al. 2012; Yun et al. 2020) and shallower sulcal depth (Ochiai et al. 2004; Van Essen 2005) compared with the right during fetal periods. Although the underlying mechanisms of prenatal cerebral asymmetry remain unknown, atypical asymmetry in the perisylvian regions is thought to be related to impairments of lateralization of language function in children (Locke 1997; Minagawa-Kawai et al. 2011; Bishop 2013). In children with DS, language deficits are one of the most distinct impairments (Chapman and Hesketh 2001; Pinter et al. 2001; Vicari 2006). Associated with deficits of auditory and language processes, decreased functional activation in superior and middle temporal gyri were also found (Losin et al. 2009; Jacola et al. 2014). Based on our finding in asymmetry analysis, the deeper sulcal depth in left superior temporal sulcus in fetuses with DS is a result of atypical asymmetry caused by earlier sulcal emergence and folding compared with TD, which is associated with impairment of language function due to DS.

Consistent observations from the abovementioned studies in fetuses, children, and adults with DS, suggest that the regional structural alterations we observed in fetal brains may persist throughout life and thus influence regional neurodevelopmental function. Fetal cerebral regions we identified with significantly different sulcal depth have critical neurodevelopmental functions that are characteristically impaired in individuals with DS compared with TD individuals (Grieco et al. 2015). Those functions (regions) include a transcortical information hub of complex multimodal information processing (insula) (Gogolla 2017), visual-motor processing (parieto-occipital) (Pitzalis et al. 2015), primary somatic motor/sensory areas (central), auditory working memory, and auditory processing (supratemporal sulcus). Those neurodevelopmental functions are also characteristically impaired in individuals with DS relative to other non-DS causes of intellectual disability such as fragile X or Williams syndromes (Grieco et al. 2015). In contrast, occipital regions did not show significant differences in sulcal depth between fetuses with DS and TD, consistent with relatively preserved visual cognitive function in DS such as visio-spatial processing (Grieco et al. 2015).

Although our findings were obtained by reliable methods and statistical approaches, there are some limitations that should be addressed in this study. First, we used a small sample size compared with other studies in children or adolescents with DS. In the fetal brain, the cortical folding pattern shows dynamic changes with increasing gestational age and regional diversity across brain areas. For more details about brain alteration in fetuses with DS, therefore, a larger sample of fetal brain MRIs should be collected and analyzed for future analysis. Second, our data included only one subject with a follow-up scan. Although we showed the regional depth differences using cross-sectional data were almost the same as those including longitudinal data, it is necessary to use more longitudinal data to generate accurate age-related trajectories of sulcal depth. Third, MRIs of fetal subjects were acquired by two different scanners (3 T Siemens from BCH, and 1.5 T Philips from TMC), which could lead to biased results in group comparison. However, our prior studies found no significant difference in the accuracy of image processing and analysis between BCH and TMC scanners (Tarui et al. 2018; Yun et al. 2019). Here, we performed a group comparison of sulcal depth in TD fetuses between different scanners using a linear regression model. After FDR correction, we found no significant scanner effect in sulcal depth (Supplementary Fig. 5). This demonstrates that our findings were not biased by the scanner. To confirm this, repeated or phantom MRI from different scanners should be acquired and analyzed in further studies. The result of the regional group comparison after adjusting GW, cerebral volume, and scanner effects is similar to the main result shown in Figure 3 (Supplementary Fig. 4). This comparison also supports the no scanner effect on our sulcal depth analysis. Moreover, it shows that group differences in sulcal depth were not affected by cerebral volume. Smaller brain volume in children with DS has been frequently reported (Pinter et al. 2001; Menghini et al. 2011; Lee et al. 2016; Hamner et al. 2018; Baburamani et al. 2019; Rodrigues et al. 2019). However, in our previous study using living fetuses, we found that whole-brain volume ($P = 0.126$) and whole cerebral volume ($P = 0.126$) were not different between fetuses with DS and TD fetuses (Tarui et al. 2020). Therefore, these results demonstrate that the findings without adjusting cerebral volume are reliable to show group difference in sulcal depth.

In conclusion, this article investigated global and regional differences in cortical folding between DS and TD fetuses. We identified several cortical regions with alterations of brain development that suggest altered neurogenesis and neuronal proliferation. The altered regions are also related to characteristic neurocognitive impairments in patients with DS. Our findings demonstrated that investigating cortical folding in the fetal brain with DS is a useful tool to detect the emergence of altered brain development and pathology in early fetal life.

Supplementary Material

Supplementary material can be found at *Cerebral Cortex* online.

Notes

Funding

References

Anderson JS, Nielsen JA, Ferguson MA, Burback MC, Cox ET, Dai L, Gerig G, Edgin JO, Korenberg JR. 2013. Abnormal brain synchrony in Down syndrome. *NeuroImage: Clinical.* 2:703–715.

Baburamani AA, Patkee PA, Arichi T, Rutherford MA. 2019. New approaches to studying early brain development in Down syndrome. *Dev Med Child Neurol.* 61:867–879.

Baltagi B. 2008. *Econometric analysis of panel data.* New York: John Wiley & Sons.

Bhattacharyya A, McMillan E, Chen SI, Wallace K, Svendsen CN. 2009. A critical period in cortical interneuron neurogenesis in Down syndrome revealed by human neural progenitor cells. *DNE.* 31:497–510.

Bishop DVM. 2013. Cerebral asymmetry and language development: cause, correlate or consequence? *Science.* 340:1230531.

Boucher M, Whitesides S, Evans A. 2009. Depth potential function for folding pattern representation, registration and analysis. *Med Image Anal.* 13:203–214.

Carducci F, Onorati P, Condoluci C, Gennaro GD, Quarato PP, Pierallini A, Sarà M, Miano S, Cornia R, Albertini G. 2013. Whole-brain voxel-based morphometry study of children and adolescents with Down syndrome. *Funct Neurol.* 10.

CDC. 2019. *Facts about Down Syndrome.* https://www.cdc.gov/ncbddd/birthdefects/downsyndrome.html (March 2020, date last accessed).

Chapman, RS, Hesketh LJ. 2001. *Language, cognition, and short-term memory in individuals with Down syndrome.* Down Syndrome Research and Practice. https://library.down-syndrome.org/en-us/research-practice/07/1/language-cognition-short-term-memory-individuals-down-syndrome/ (March 2020, date last accessed).

Chen C-H, Gutierrez ED, Thompson W, Panizzon MS, Jernigan TL, Eyler LT, Fennema-Notestine C, Jak AJ, Neale MC, Franz CE *et al.* 2012. Hierarchical genetic Organization of Human Cortical Surface Area. *Science.* 335:1634.

Chen CY, Zimmerman RA, Faro S, Parrish B, Wang Z, Bilaniuk LT, Chou TY. 1996. MR of the cerebral operculum: abnormal opercular formation in infants and children. *Am J Neuroradiol.* 17:1303–1311.

Chenn A, Walsh CA. 2002. Regulation of cerebral cortical size by control of cell cycle exit in neural precursors. *Science.* 297:365–369.

Clouchoux C, Kudelski D, Gholipour A, Warfield SK, Viseur S, Bouyssi-Kobar M, Mari J-L, Evans AC, du Plessis AJ, Limperopoulos C. 2012. Quantitative in vivo MRI measurement of cortical development in the fetus. *Brain Struct Funct.* 217:127–139.

Cykowski MD, Coulon O, Kochunov PV, Amunts K, Lancaster JL, Laird AR, Glahn DC, Fox PT. 2008. The central sulcus: an observer-independent characterization of sulcal landmarks and depth asymmetry. *Cereb Cortex.* 18:1999–2009.

Davis WE, Kelso JA. 1982. Analysis of "invariant characteristics" in the motor control of down's syndrome and normal subjects. *J Mot Behav.* 14:194–212.

Dubois J, Benders M, Cachia A, Lazeyras F, Ha-Vinh Leuchter R, Sizonenko SV, Borradori-Tolsa C, Mangin JF, Hüppi PS. 2008. Mapping the early cortical folding process in the preterm newborn brain. *Cereb Cortex.* 18:1444–1454.

Eickhoff SB, Heim S, Zilles K, Amunts K. 2006. Testing anatomically specified hypotheses in functional imaging using cytoarchitectonic maps. *Neuroimage.* 32:570–582.

Engelhardt E, Inder TE, Alexopoulos D, Dierker DL, Hill J, Van Essen D, Neil JJ. 2015. Regional impairments of cortical folding in premature infants. *Ann Neurol.* 77:154–162.

Fischl B, Rajendran N, Busa E, Augustinack J, Hinds O, Yeo BTT, Mohlberg H, Amunts K, Zilles K. 2008. Cortical folding patterns and predicting cytoarchitecture. *Cereb Cortex.* 18:1973–1980.

Garel C, Chantrel E, Brisse H, Elmaleh M, Luton D, Oury JF, Sebag G, Hassan M. 2001. Fetal cerebral cortex: normal gestational landmarks identified using prenatal MR imaging. *AJNR Am J Neuroradiol.* 22:184–189.

Garel C, Chantrel E, Elmaleh M, Brisse H, Sebag G. 2003. Fetal MRI: normal gestational landmarks for cerebral biometry, gyration and myelination. *Childs Nerv Syst.* 19:422–425.

Gaser C, Luders E, Thompson PM, Lee AD, Dutton RA, Geaga JA, Hayashi KM, Bellugi U, Galaburda AM, Korenberg JR *et al.* 2006. Increased local gyrification mapped in Williams syndrome. *Neuroimage.* 33:46–54.

Germann J, Chakravarty MM, Collins LD, Petrides M. 2019. Tight coupling between morphological features of the central sulcus and somatomotor body representations: a combined anatomical and functional MRI study. *Cereb Cortex.* bhz208.

Germann J, Robbins S, Halsband U, Petrides M. 2005. Precentral sulcal complex of the human brain: morphology and statistical probability maps. *J Comp Neurol.* 493:334–356.

Gogolla N. 2017. The insular cortex. *Curr Biol.* 27:R580–R586.

Golden JA, Hyman BT. 1994. Development of the superior temporal neocortex is anomalous in trisomy 21. *J Neuropathol Exp Neurol.* 53:513–520.

Grieco J, Pulsifer M, Seligsohn K, Skotko B, Schwartz A. 2015. Down syndrome: cognitive and behavioral functioning across the lifespan. *Am J Med Genet C Semin Med Genet.* 169:135–149.

Guibaud L, Selleret L, Larroche JC, Buenerd A, Alias F, Gaucherand P, Portes VD, Pracros J-P. 2008. Abnormal Sylvian fissure on prenatal cerebral imaging: significance and correlation with neuropathological and postnatal data. *Ultrasound Obstet Gynecol.* 32:50–60.

Guidi S, Bonasoni P, Ceccarelli C, Santini D, Gualtieri F, Ciani E, Bartesaghi R. 2008. Neurogenesis impairment and increased cell death reduce Total neuron number in the hippocampal region of Fetuses with Down syndrome. *Brain Pathol.* 18:180–197.

Guidi S, Giacomini A, Stagni F, Emili M, Uguagliati B, Bonasoni MP, Bartesaghi R. 2018. Abnormal development of the inferior temporal region in fetuses with Down syndrome. *Brain Pathol.* 28:986–998.

Guihard-Costa A-M, Khung S, Delbecque K, Ménez F, Delezoide A-L. 2006. Biometry of face and brain in fetuses with trisomy 21. *Pediatr Res.* 59:33–38.

Habas PA, Scott JA, Roosta A, Rajagopalan V, Kim K, Rousseau F, Barkovich AJ, Glenn OA, Studholme C. 2012. Early folding patterns and asymmetries of the normal human brain detected from in utero MRI. *Cereb Cortex.* 22:13–25.

Hamner T, Udhnani MD, Osipowicz KZ, Lee NR. 2018. Pediatric brain development in Down syndrome: a field in its infancy. *J Int Neuropsychol Soc*. 24:966–976.

Harris JM, Yates S, Miller P, Best JJK, Johnstone EC, Lawrie SM. 2004. Gyrification in first-episode schizophrenia: a morphometric study. *Biol Psychiatry*. 55:141–147.

Hasnain MK, Fox PT, Woldorff MG. 2001. Structure–function spatial covariance in the human visual cortex. *Cereb Cortex*. 11:702–716.

Hill J, Inder T, Neil J, Dierker D, Harwell J, Van Essen D. 2010. Similar patterns of cortical expansion during human development and evolution. *Proc Natl Acad Sci U S A*. 107: 13135–13140.

Im K, Guimaraes A, Kim Y, Cottrill E, Gagoski B, Rollins C, Ortinau C, Yang E, Grant PE. 2017. Quantitative folding pattern analysis of early primary sulci in human fetuses with brain abnormalities. *AJNR Am J Neuroradiol*. 38:1449–1455.

Jacola LM, Byars AW, Hickey F, Vannest J, Holland SK, Schapiro MB. 2014. Functional magnetic resonance imaging of story listening in adolescents and young adults with Down syndrome: evidence for atypical neurodevelopment. *J Intellect Disabil Res*. 58:892–902.

Kanaumi T, Milenkovic I, Adle-Biassette H, Aronica E, Kovacs GG. 2013. Non-neuronal cell responses differ between normal and Down syndrome developing brains. *Int J Dev Neurosci*. 31:796–803.

Kates WR, Folley BS, Lanham DC, Capone GT, Kaufmann WE. 2002. Cerebral growth in fragile X syndrome: review and comparison with Down syndrome. *Microsc Res Tech*. 57:159–167.

Kostovic I, Vasung L. 2009. Insights from in vitro fetal magnetic resonance imaging of cerebral development. *Semin Perinatol*. 33:220–233.

Kuklisova-Murgasova M, Quaghebeur G, Rutherford MA, Hajnal JV, Schnabel JA. 2012. Reconstruction of fetal brain MRI with intensity matching and complete outlier removal. *Med Image Anal*. 16:1550–1564.

Lee NR, Adeyemi EI, Lin A, Clasen LS, Lalonde FM, Condon E, Driver DI, Shaw P, Gogtay N, Raznahan A *et al*. 2016. Dissociations in cortical morphometry in youth with Down syndrome: evidence for reduced surface area but increased thickness. *Cereb Cortex*. 26:2982–2990.

Lefèvre J, Germanaud D, Dubois J, Rousseau F, de Macedo Santos I, Angleys H, Mangin J-F, Hüppi PS, Girard N *et al*. 2016. Are developmental trajectories of cortical folding comparable between cross-sectional datasets of fetuses and preterm newborns? *Cereb Cortex*. 26:3023–3035.

Lerman-Sagie T, Malinger G. 2008. Focus on the fetal Sylvian fissure. *Ultrasound Obstet Gynecol*. 32:3–4.

Leroy F, Cai Q, Bogart SL, Dubois J, Coulon O, Monzalvo K, Fischer C, Glasel H, Van der Haegen L, Bénézit A *et al*. 2015. New human-specific brain landmark: the depth asymmetry of superior temporal sulcus. *Proc Natl Acad Sci U S A*. 112:1208–1213.

Locke JL. 1997. A theory of neurolinguistic development. *Brain Lang*. 58:265–326.

Losin EA, Rivera SM, O'Hare ED, Sowell ER, Pinter JD. 2009. Abnormal fMRI activation pattern during story listening in individuals with Down syndrome. *Am J Intellect Dev Disabil*. 114:369–380.

Lui JH, Hansen DV, Kriegstein AR. 2011. Development and evolution of the human neocortex. *Cell*. 146:18–36.

Mai CT, Isenburg JL, Canfield MA, Meyer RE, Correa A, Alverson CJ, Lupo PJ, Riehle-Colarusso T, Cho SJ, Aggarwal D *et al*. 2019. National population-based estimates for major birth defects, 2010–2014. *Birth Defects Research*. 111:1420–1435.

Marcell. 1995. *Relationships Between Hearing and Auditory Cognition in Down Syndrome Youth*. Down Syndrome Research and Practice. https://library.down-syndrome.org/en-gb/research-practice/03/3/relationships-hearing-auditory-cognition-down-syndrome-youth/ (March 2020, date last accessed).

McKay DR, Kochunov P, Cykowski MD, Kent JW, Laird AR, Lancaster JL, Blangero J, Glahn DC, Fox PT. 2013. Sulcal depth-position profile is a genetically mediated neuroscientific trait: description and characterization in the central sulcus. *J Neurosci*. 33:15618–15625.

Menghini D, Costanzo F, Vicari S. 2011. Relationship between brain and cognitive processes in Down syndrome. *Behav Genet*. 41:381–393.

Meyer M, Desbrun M, Schröder P, Barr AH. 2003. Discrete differential-geometry operators for triangulated 2-manifolds. In: *Visualization and mathematics III. Mathematics and visualization*. Berlin, Heidelberg: Springer, p. 35–57.

Miller JA, Ding S-L, Sunkin SM, Smith KA, Ng L, Szafer A, Ebbert A, Riley ZL, Royall JJ, Aiona K *et al*. 2014. Transcriptional landscape of the prenatal human brain. *Nature*. 508: 199–206.

Minagawa-Kawai Y, Cristià A, Dupoux E. 2011. Cerebral lateralization and early speech acquisition: a developmental scenario. *Dev Cogn Neurosci*. 1:217–232.

Molko N, Cachia A, Rivière D, Mangin JF, Bruandet M, Le Bihan D, Cohen L, Dehaene S. 2003. Functional and structural alterations of the intraparietal sulcus in a developmental dyscalculia of genetic origin. *Neuron*. 40:847–858.

Nakamura M, Nestor PG, McCarley RW, Levitt JJ, Hsu L, Kawashima T, Niznikiewicz M, Shenton ME. 2007. Altered orbitofrontal sulcogyral pattern in schizophrenia. *Brain*. 130:693–707.

Nordahl CW, Dierker D, Mostafavi I, Schumann CM, Rivera SM, Amaral DG, Van Essen DC. 2007. Cortical folding abnormalities in autism revealed by surface-based morphometry. *J Neurosci*. 27:11725–11735.

Ochiai T, Grimault S, Scavarda D, Roch G, Hori T, Rivière D, Mangin JF, Régis J. 2004. Sulcal pattern and morphology of the superior temporal sulcus. *Neuroimage*. 22:706–719.

O'Leary DDM, Chou S-J, Sahara S. 2007. Area patterning of the mammalian cortex. *Neuron*. 56:252–269.

Palisano RJ, Walter SD, Russell DJ, Rosenbaum PL, Gémus M, Galuppi BE, Cunningham L. 2001. Gross motor function of children with Down syndrome: creation of motor growth curves. *Arch Phys Med Rehabil*. 82:494–500.

Patkee PA, Baburamani AA, Kyriakopoulou V, Davidson A, Avini E, Dimitrova R, Allsop J, Hughes E, Kangas J, McAlonan G *et al*. 2020. Early alterations in cortical and cerebellar regional brain growth in Down syndrome: an in vivo fetal and neonatal MRI assessment. *NeuroImage: Clinical*. 25:102139.

Piao X, Hill RS, Bodell A, Chang BS, Basel-Vanagaite L, Straussberg R, Dobyns WB, Qasrawi B, Winter RM, Innes AM *et al*. 2004. G protein-coupled receptor-dependent development of human frontal cortex. *Science*. 303:2033–2036.

Pinter JD, Eliez S, Schmitt JE, Capone GT, Reiss AL. 2001. Neuroanatomy of Down's syndrome: a high-resolution MRI study. *AJP*. 158:1659–1665.

Pitzalis S, Fattori P, Galletti C. 2015. The human cortical areas V6 and V6A. *Vis Neurosci*. 32:E007.

Rakic P. 1988. Specification of cerebral cortical areas. *Science*. 241:170–176.

Rakic P. 2004. Genetic control of cortical convolutions. *Science*. 303:1983–1984.

Rakic P. 2009. Evolution of the neocortex: a perspective from developmental biology. *Nat Rev Neurosci*. 10:724–735.

Ramenghi LA, Fumagalli M, Righini A, Bassi L, Groppo M, Parazzini C, Bianchini E, Triulzi F, Mosca F. 2007. Magnetic resonance imaging assessment of brain maturation in preterm neonates with punctate white matter lesions. *Neuroradiology*. 49:161–167.

Rigoldi C, Galli M, Condoluci C, Carducci F, Onorati P, Albertini G. 2009. Gait analysis and cerebral volumes in Down's syndrome. *Funct Neurol*. 24:147–152.

Robbins S, Evans AC, Collins DL, Whitesides S. 2004. Tuning and comparing spatial normalization methods. *Med Image Anal*. 8:311–323.

Robbins SM. 2004. *Anatomical standardization of the human brain in euclidean 3-space and on the cortical 2-manifold*. Canada: McGill University.

Rodrigues M, Nunes J, Figueiredo S, Martins de Campos A, Geraldo AF. 2019. Neuroimaging assessment in Down syndrome: a pictorial review. *Insights Imaging*. 10:52.

Ronan L, Fletcher PC. 2015. From genes to folds: a review of cortical gyrification theory. *Brain Struct Funct*. 220:2475–2483.

Rubenstein JLR, Rakic P. 1999. Genetic control of cortical development. *Cereb Cortex*. 9:521–523.

Schaer M, Schmitt JE, Glaser B, Lazeyras F, Delavelle J, Eliez S. 2006. Abnormal patterns of cortical gyrification in velo-cardio-facial syndrome (deletion 22q11.2): an MRI study. *Psychiatry Res*. 146:1–11.

Serag A, Kyriakopoulou V, Rutherford MA, Edwards AD, Hajnal JV, Aljabar P, Counsell SJ, Boardman JP, Rueckert D. 2012. A multi-channel 4D probabilistic atlas of the developing brain: application to Fetuses and neonates. 2012:14.

Shimony JS, Smyser CD, Wideman G, Alexopoulos D, Hill J, Harwell J, Dierker D, Van Essen DC, Inder TE, Neil JJ. 2016. Comparison of cortical folding measures for evaluation of developing human brain. *Neuroimage*. 125:780–790.

Stagni F, Giacomini A, Emili M, Guidi S, Bartesaghi R. 2018. Neurogenesis impairment: an early developmental defect in Down syndrome. *Free Radic Biol Med*. 114:15–32.

Stahl R, Walcher T, De Juan Romero C, Pilz GA, Cappello S, Irmler M, Sanz-Aquela JM, Beckers J, Blum R, Borrell V *et al*. 2013. Trnp1 regulates expansion and folding of the mammalian cerebral cortex by control of radial glial fate. *Cell*. 153:535–549.

Sun T, Hevner RF. 2014. Growth and folding of the mammalian cerebral cortex: from molecules to malformations. *Nat Rev Neurosci*. 15:217–232.

Tarui T, Im K, Madan N, Madankumar R, Skotko BG, Schwartz A, Sharr C, Ralston SJ, Kitano R, Akiyama S *et al*. 2020. Quantitative MRI analyses of regional brain growth in living Fetuses with Down syndrome. *Cereb Cortex*. 30:382–390.

Tarui T, Madan N, Farhat N, Kitano R, Ceren Tanritanir A, Graham G, Gagoski B, Craig A, Rollins CK, Ortinau C *et al*. 2018. Disorganized patterns of sulcal position in fetal brains with agenesis of corpus callosum. *Cereb Cortex*. 28:3192–3203.

Van Essen DC. 2005. A population-average, landmark- and surface-based (PALS) atlas of human cerebral cortex. *Neuroimage*. 28:635–662.

Vicari S. 2006. Motor development and neuropsychological patterns in persons with Down syndrome. *Behav Genet*. 36:355–364.

Welker W. 1990. Why does cerebral cortex fissure and fold? In: *Cerebral Cortex*. *Cerebral Cortex*. Boston, MA: Springer, p. 3–136.

White T, Su S, Schmidt M, Kao C-Y, Sapiro G. 2010. The development of gyrification in childhood and adolescence. *Brain Cogn*. 72:36–45.

Yun HJ, Chung AW, Vasung L, Yang E, Tarui T, Rollins CK, Ortinau CM, Grant PE, Im K. 2019. Automatic labeling of cortical sulci for the human fetal brain based on spatio-temporal information of gyrification. *Neuroimage*. 188:473–482.

Yun HJ, Im K, Yang J-J, Yoon U, Lee J-M. 2013. Automated Sulcal depth measurement on cortical surface reflecting geometrical properties of sulci. *Plos One*. 8:e55977.

Yun HJ, Vasung L, Tarui T, Rollins CK, Ortinau CM, Grant PE, Im K. 2020. Temporal patterns of emergence and spatial distribution of Sulcal pits during Fetal life. *Cereb Cortex*. 30:4257–4268.

Zilles K, Armstrong E, Schleicher A, Kretschmann HJ. 1988. The human pattern of gyrification in the cerebral cortex. *Anat Embryol*. 179:173–179.

Zilles K, Schleicher A, Langemann C, Amunts K, Morosan P, Palomero-Gallagher N, Schormann T, Mohlberg H, Bürgel U, Steinmetz H *et al*. 1997. Quantitative analysis of sulci in the human cerebral cortex: development, regional heterogeneity, gender difference, asymmetry, intersubject variability and cortical architecture. *Hum Brain Mapp*. 5:218–221.